Tree Physiology 00, 1–15
https://doi.org/10.1093/treephys/tpac049

Research paper

Cell-level anatomy explains leaf age-dependent declines in mesophyll conductance and photosynthetic capacity in the evergreen Mediterranean oak *Quercus ilex* subsp. *rotundifolia*

David Alonso-Forn[1], José Javier Peguero-Pina[1,2,6], Juan Pedro Ferrio[1,3], José Ignacio García-Plazaola[4], Rubén Martín-Sánchez[1], Ülo Niinemets[5], Domingo Sancho-Knapik[1,2] and Eustaquio Gil-Pelegrín[1]

[1]Departamento de Sistemas Agrícolas, Forestales y Medio Ambiente, Centro de Investigación y Tecnología Agroalimentaria de Aragón (CITA), Avda Montañana 930, Zaragoza 50059, Spain; [2]Instituto Agroalimentario de Aragón -IA2- (CITA-Universidad de Zaragoza), Zaragoza, Spain; [3]Aragon Agency for Research and Development (ARAID), Zaragoza E-50018, Spain; [4]Department of Plant Biology and Ecology, University of the Basque Country (UPV/EHU), Apdo 644, Bilbao 48080, Spain; [5]Crop Science and Plant Biology, Estonian University of Life Sciences, Kreutzwaldi 1, 51006 Tartu, Estonia; [6]Corresponding author (jjpeguero@aragon.es)

Received January 11, 2022; accepted April 13, 2022; handling Editor Antonio Diaz-Espejo

Leaves of Mediterranean evergreen tree species experience a reduction in net CO_2 assimilation (A_N) and mesophyll conductance to CO_2 (g_m) during aging and senescence, which would be influenced by changes in leaf anatomical traits at cell level. Anatomical modifications can be accompanied by the dismantling of photosynthetic apparatus associated to leaf senescence, manifested through changes at the biochemical level (i.e., lower nitrogen investment in photosynthetic machinery). However, the role of changes in leaf anatomy at cell level and nitrogen content in g_m and A_N decline experienced by old non-senescent leaves of evergreen trees with long leaf lifespan is far from being elucidated. We evaluated age-dependent changes in morphological, anatomical, chemical and photosynthetic traits in *Quercus ilex* subsp. *rotundifolia* Lam., an evergreen oak with high leaf longevity. All photosynthetic traits decreased with increasing leaf age. The relative change in cell wall thickness (T_{cw}) was less than in chloroplast surface area exposed to intercellular air space (S_c/S), and S_c/S was a key anatomical trait explaining variations in g_m and A_N among different age classes. The reduction of S_c/S was related to ultrastructural changes in chloroplasts associated to leaf aging, with a concomitant reduction in cytoplasmic nitrogen. Changes in leaf anatomy and biochemistry were responsible for the age-dependent modifications in g_m and A_N. These findings revealed a gradual physiological deterioration related to the dismantling of the photosynthetic apparatus in older leaves of *Q. ilex* subsp. *rotundifolia*.

Keywords: holm oak, leaf aging, leaf anatomy, mesophyll conductance, nitrogen, photosynthesis.

Introduction

The ecological implications of differences in leaf lifespan have been analyzed by cost–benefit models that optimize leaf lifetime carbon gain in different environments (Chabot and Hicks 1982, Kikuzawa 1991, Ackerly 1999). These models postulate that leaves should be replaced when leaf maintenance costs during unfavorable periods surpass the carbon gain in favorable periods or, alternatively, the potential future gain is less than the cost of losing the leaves in terms of carbon and nutrient investment (Chabot and Hicks 1982). It is widely acknowledged that developing leaves show a rise in photosynthesis to maximum levels that is followed by an age-dependent decrease in photosynthetic potential until leaf senescence (Freeland 1952, Chabot and Hicks 1982, Niinemets et al. 2004, 2006, 2009, 2012, Harayama et al. 2016).

Evergreen tree species with long leaf lifespan retain several cohorts of foliage that can contribute significantly to canopy photosynthesis (Niinemets et al. 2005, Warren 2006,

Peguero-Pina et al. 2007, Yasumura and Ishida 2011). Indeed, Escudero and Mediavilla (2003) analyzed the decline in photosynthetic performance of several evergreen species from Mediterranean-type climates with long lifespan, concluding that the retention of old leaves resulted in a higher whole-canopy net CO_2 assimilation, despite their lower assimilation rate.

Studies have also found evidence for increased photosynthetic limitation in older leaves of different plant species due to a reduced mesophyll conductance to CO_2 (g_m) (Loreto et al. 1994, Flexas et al. 2007*a*, Zhang et al. 2008, Niinemets et al. 2009), including Mediterranean evergreen tree species during aging and senescence (Niinemets et al. 2005, 2006). In fact, g_m plays a predominant role in the photosynthetic process of Mediterranean evergreen tree species, being often the most limiting factor for net CO_2 assimilation (Flexas et al. 2014, Galmés et al. 2014, Niinemets and Keenan 2014, Peguero-Pina et al. 2016*a*, Peguero-Pina et al. 2017*a*, Peguero-Pina et al. 2018, Alonso-Forn et al. 2021).

Values of g_m for a given plant species can be influenced by different leaf anatomical traits, mainly the cell wall thickness, the mesophyll and chloroplast surface area exposed to intercellular air space per unit leaf area (S_m/S and S_c/S, respectively) and the chloroplast size (Terashima et al. 2011, Tomás et al. 2013, Peguero-Pina et al. 2016*b*, 2017*b*, Sáez et al. 2017, Sáez et al. 2018, Carriquí et al. 2019). Given the strong control of leaf anatomy on g_m, Niinemets et al. (2005) suggested that the drawdown of photosynthesis and g_m in older leaves of Mediterranean evergreen tree species could be associated with increases in the thickness of mesophyll cell walls with increasing leaf age. Moreover, Niinemets et al. (2009) proposed that the dismantling of the photosynthetic apparatus associated to leaf senescence would reduce S_c/S, which could explain the reduction of both g_m and net CO_2 assimilation. Recently, Clarke et al. (2021) concluded that reduced g_m in older leaves of the annual forb *Nicotiana tabacum* was associated with cell wall thickening and reduction in S_c/S. However, to the best of our knowledge, there is a lack of empirical studies of age-dependent changes in leaf anatomical traits (i.e., cell wall thickness, S_c/S, chloroplast number and size) as the mechanistic explanation for the decline in photosynthetic potential of older leaves in species with long leaf lifespan.

Moreover, the dismantling of photosynthetic apparatus associated to leaf senescence can be manifested through a decrease in leaf nitrogen content and/or lower fractions of nitrogen in photosynthetic enzymes of functional chloroplasts (i.e., Rubisco and rate-limiting components of photosynthetic electron transport). Reallocation of N from older to younger leaves has been interpreted as a mechanism to improve whole-canopy photosynthesis (Thomas and Stoddart 1980, Chabot and Hicks 1982, Field 1983, Field and Mooney 1983, Smart 1994, Kitajima et al. 1997). Indeed, Warren (2006) and Kuusk et al. (2018) found that the concentrations of nitrogen and the maximum rate of carboxylation (V_{cmax}) decreased with needle age in different *Pinus* species. On the other hand, Hikosaka (2005) suggested that the decrease in photosynthetic potential in evergreen species with a longer leaf lifespan is not necessarily coupled with leaf nitrogen content. In this regard, Niinemets et al. (2005) only found minor changes in nitrogen content per unit area in older leaves of Mediterranean evergreens despite the fact that the capacities for photosynthetic electron transport (J_{max}) and V_{cmax} decreased fivefold on an area basis.

Therefore, the role of leaf anatomy and nitrogen content in determining g_m and photosynthetic capacity in old non-senescent leaves of evergreen trees with long leaf lifespan is far from being elucidated. We hypothesized that (i) changes in leaf anatomical traits (e.g., increased cell wall thickness and/or decreased S_c/S) in older leaves of evergreen species with long leaf lifespan are primarily responsible for decreases in foliage photosynthetic potentials in older leaves and (ii) anatomical modifications are accompanied by age-dependent changes at biochemical level (e.g., the decrease in nitrogen investment in photosynthetic machinery). To test these hypotheses, we evaluated the age-dependent changes in morphological, anatomical, chemical and photosynthetic traits in *Q. ilex* subsp. *rotundifolia* Lam., a Mediterranean evergreen oak with high leaf longevity (ca 28 months, according to Mediavilla and Escudero 2003) and a high fraction of leaves >1 year old that play an important role in canopy photosynthesis (Sala i Serra 1992, Corcuera et al. 2005).

Materials and methods

Plant material and experimental conditions

This study was carried out with adult ca 5 m tall trees of *Q. ilex* subsp. *rotundifolia* ('Cazorla' provenance, seed origin: 38°06′ N, 02°33′ W, 1236 m above sea level, Spain) growing outdoors at CITA de Aragón (41°39′ N, 0°52′ W, Zaragoza, Spain) under Mediterranean conditions (mean annual temperature 15.4 °C, total annual precipitation 298 mm). All trees were exposed to the same environmental conditions and drip-irrigated every 2 days. Physiological measurements were carried out in September 2018 in current-year (0-year-old), 1-year-old and 2-year-old leaves from three branches of three 15-year-old trees. The same measurements were repeated during September 2020 in current-year (0-year-old), 1-year-old and 2-year-old leaves from the same three branches of the same trees. Thus, the current-year leaves (0-year-old) measured in September 2018 correspond to the 2-year-old leaves measured in September 2020.

Light environment was characterized with three HOBO Pendant temp/light sensors (ONSET, Bourne, MA, USA) placed along a branch to determine the average light intensity above each of the three leaf cohorts studied (0-year-old, 1-year-old and 2-year-old). Measurements were recorded every 1 min

during three sunny days of September 2018 (Figure S1 available as Supplementary data at *Tree Physiology* Online). The integrated daily quantum flux density (Q_{int}, mol m^{-2} day^{-1}) was calculated for each leaf cohort from the mean values of incident solar radiation (Cescatti and Zorer 2003) (Figure S2 available as Supplementary data at *Tree Physiology* Online).

Leaf gas-exchange and chlorophyll fluorescence measurements

Simultaneous gas-exchange and chlorophyll fluorescence measurements were carried out between 09:00 and 10:00 h (solar time) with a portable photosystem system CIRAS-2 (PP-Systems, Amesbury, MA, USA) fitted with an automatic universal leaf cuvette (PLC6-U, PP-Systems) and an FMS II portable pulse amplitude modulated fluorometer (Hansatech Instruments Ltd, Norfolk, UK). All measurements were conducted under the following standard environmental conditions: CO_2 concentration surrounding the leaf (C_a) of 400 μmol mol^{-1}, leaf temperature of 25 °C, vapor pressure deficit of 1.25 kPa and saturating photosynthetic photon flux density (PPFD) of 1500 μmol m^{-2} s^{-1}. Additional measurements were also performed under lower PPFD of 350 and 750 μmol m^{-2} s^{-1} in September 2018. After steady state gas-exchange rate was reached, the net assimilation rate (A_N), the stomatal conductance (g_s) and the effective quantum yield of PSII (Φ_{PSII}) were estimated. Φ_{PSII} was calculated as $(F'_M-F_S)/F'_M$, where F_S is the steady-state fluorescence yield and F'_M is the maximum fluorescence yield during an 1 s saturating light pulse of ca 8000 μmol m^{-2} s^{-1} (Genty et al. 1989). Photosynthetic electron transport rate (J_{flu}) was then calculated according to Krall and Edwards (1992), following the methodology described in Peguero-Pina et al. (2016*a*). Leakage of CO_2 in and out of the cuvette was determined for the same range of CO_2 concentrations as described in Flexas et al. (2007*b*) and used to correct the values of A_N and corresponding substomatal CO_2 concentration (C_i).

Estimation of mesophyll conductance, g_m and maximum velocity of carboxylation (V_{cmax}) by gas exchange and chlorophyll fluorescence

Mesophyll conductance (g_m) and maximum velocity of carboxylation (V_{cmax}) were estimated according to the variable *J* method of Harley et al. (1992) (Eq. (1)) and the one-point method of De Kauwe et al. (2016) (Eq. (2)), respectively, as follows:

$$g_m = \frac{A_N}{C_i - \frac{\Gamma^*(J_F+8(A_N+R_L))}{J_F-4(A_N+R_L)}} \quad (1)$$

$$V_{cmax} = \frac{A_N}{\left(\frac{C_i-\Gamma^*}{C_i+K_m}\right) - 0.015} \quad (2)$$

where A_N and C_i values used correspond to the gas-exchange measurements at saturating light. The chloroplastic CO_2 compensation point in the absence of mitochondrial respiration (Γ^*) and the respiration rate in the light (R_L) were estimated as in Flexas et al. (2007*a*), whereas K_m (the effective Michaelis–Menten constant) was estimated as in De Kauwe et al. (2016).

Morphological and anatomical measurements and leaf nitrogen concentration

Sections of 1 mm × 1 mm were cut between the main veins from the same leaves used for gas-exchange and processed for anatomical measurements following the methodology described in Peguero-Pina et al. (2016*c*). Semi-thin (0.8 μm) and ultra-thin (90 nm) cross-sections were cut with an ultramicrotome (Reichert and Jung model Ultracut E). Semi-thin cross-sections were stained with 1% toluidine blue and viewed under a light microscope (Optika B-600TiFL, Optika Microscopes, Ponteranica, Italy). Ultrathin cross-sections were contrasted with uranyl acetate and lead citrate and viewed under a transmission electron microscope (H600, Hitachi, Tokyo, Japan). Light and electron microscopy images were analyzed with ImageJ software (http://rsb.info.nih.gov/nih-image/) to determine leaf anatomical characteristics. Light micrographs were used to measure leaf thickness, mesophyll thickness between the two epidermal layers, number of palisade layers, fraction of the mesophyll tissue occupied by the intercellular air spaces (f_{ias}), and mesophyll (S_m/S) and chloroplast (S_c/S) surface area facing intercellular air spaces per leaf area (Evans et al. 1994, Syvertsen et al. 1995, Tomás et al. 2013). Electron micrographs were used to measure the cell wall thickness (T_{cw}), cytoplasm thickness (T_{cyt}), chloroplast length (L_{chl}) and chloroplast thickness (T_{chl}) (Tomás et al. 2013). Moreover, total chloroplast area (A_{chl}) and total area occupied by starch grains and plastoglobuli (A_{st} and A_{plg}, respectively) were also measured to estimate the percentage of functional area per chloroplast as $(A_{chl}-A_{stg}-A_{plg})$ × 100. Each anatomical trait was measured in three different sections and four to six different fields of view.

Leaf dry mass per unit area (LMA) was measured in September 2018 and September 2020 in nine leaves per cohort from the same branches previously used for gas exchange and chlorophyll fluorescence measurements (three leaves of each age from each of the three trees used for measurements). Leaf area was measured after scanning the leaves with the ImageJ software. Leaf dry mass was determined after leaves were oven dried at 70 °C for 3 days. The LMA was calculated as the ratio of foliage dry mass to foliage area.

Total leaf nitrogen (N_{total}) was quantified in dried leaves using an Organic Elemental Analyzer (Flash EA 112, Thermo Fisher Scientific Inc., Waltham, MA, USA). For the leaves measured in September 2020, the cell wall fraction was obtained after performing the neutral fiber detergent (NDF) following the method of Goering and Van Soest (1970). Nitrogen content of the cell wall fraction ($N_{cell\ wall}$) was further estimated using the elemental analyzer as aforementioned. The fraction of nitrogen

allocated in the cytoplasm ($N_{cytoplasm}$) was calculated as follows: $N_{cytoplasm} = (N_{total} \times 100 – N_{cell\ wall} \times NDF)/(100 – NDF)$.

Mesophyll conductance modeled on the basis of anatomical traits

Mesophyll diffusion conductance estimated using the measured leaf anatomical traits ($g_{m,a}$) was calculated as a composite conductance of within-leaf gas and liquid diffusion pathways, according to the one-dimensional gas diffusion model of Niinemets and Reichstein (2003) as applied by Tosens et al. (2012):

$$g_{m,a} = \frac{1}{\frac{1}{g_{ias}} + \frac{R \bullet T_k}{H \bullet g_{liq}}} \quad (3)$$

where g_{ias} is the gas phase conductance from substomatal cavities to outer surface of cell walls, g_{liq} is the conductance in the liquid and lipid phases from the outer surface of cell walls to chloroplasts, R is the gas constant (Pa m^3 K^{-1} mol^{-1}), T_k is the absolute temperature (K) and H is the Henry's law constant for CO_2 (Pa m^3 mol^{-1}). $g_{m,a}$ is defined as a gas-phase conductance, and thus $H/(RT_k)$, the dimensionless form of the Henry's law constant converts g_{liq} to the corresponding gas-phase equivalent conductance (Niinemets and Reichstein 2003).

The gas-phase conductance (and the reciprocal term, r_{ias}) was calculated as described in Niinemets and Reichstein (2003):

$$g_{ias} = \frac{1}{r_{ias}} = \frac{D_A \bullet f_{ias}}{\Delta L_{ias} \bullet \tau} \quad (4)$$

where ΔL_{ias} (m) is the average gas-phase thickness, τ is the diffusion path tortuosity (1.57 m m^{-1}, Syvertsen et al. 1995), D_A is the diffusivity of the CO_2 in the air ($1.51 \cdot 10^{-5}$ m^2 s^{-1} at 25 °C) and f_{ias} is the fraction of intercellular air spaces. ΔL_{ias} was taken as the half of the mesophyll thickness. Total liquid phase conductance (g_{liq}) from the outer surface of cell walls to the carboxylation sites in the chloroplasts is the sum of serial resistances of the cell wall (r_{cw}), the plasmalemma (r_{pl}) and the liquid phase inside the cell ($r_{cel,tot}$) (Tomás et al. 2013):

$$g_{liq} = \frac{S_m}{(r_{cw} + r_{pl} + r_{cel,tot}) \bullet S} \quad (5)$$

Cell wall conductance was calculated as described in Peguero-Pina et al. (2012). We used a value of 0.028 for the porosity of cell wall as previously estimated by Tomás et al. (2013) for *Q. ilex*. We used an estimate of 0.0035 m s^{-1} for the conductance of plasma membrane (Tosens et al. 2012). The conductance inside the cell was calculated considering two different pathways of CO_2 (one for cell wall parts lined with chloroplasts and the other for interchloroplastial areas, Tholen et al. 2012) as described by Tomás et al. (2013).

Quantitative limitations analyses of A_N

The relative controls on A_N were separated into their functional components according to the quantitative limitation analysis of Grassi and Magnani (2005) as applied in Tomás et al. (2013). This methodology allows comparing relative changes in limitations to net CO_2 assimilation into limitations due to limited g_s to CO_2 ($g_{s,CO2}$; stomatal limitations, l_s), g_m (mesophyll limitations, l_m) and leaf biochemistry (biochemical limitations, l_b). Each of the three components, l_s, l_m and l_b, can vary between zero and one ($l_s + l_m + l_b = 1$). They were calculated as:

$$l_s = \frac{g_{tot}/g_{s,CO2} \bullet \delta A_N/\delta C_c}{g_{tot} + \delta A_N/\delta C_c} \quad (6)$$

$$l_m = \frac{g_{tot}/g_m \bullet \delta A_N/\delta C_c}{g_{tot} + \delta A_N/\delta C_c} \quad (7)$$

$$l_b = \frac{g_{tot}}{g_{tot} + \delta A_N/\delta C_c} \quad (8)$$

where g_{tot} is the total conductance to CO_2 from leaf surface to carboxylation sites in the chloroplasts ($1/g_{tot} = 1/g_{s,CO2} + 1/g_m$). The values of g_m (Eq. (1)) were used to calculate the chloroplastic CO_2 concentration (C_c) as $C_c = C_i – A_N/g_m$. $\delta A_N/\delta C_c$ was calculated as the slope of the relationship between C_c and A_N, considering a C_c range of 50–100 μmol mol^{-1}.

Chlorophyll measurements

Discs from the leaves measured in September 2020 were wrapped in aluminum foil, frozen in liquid nitrogen and stored at −20 °C. Pigments were extracted with acetone (100%) in presence of Na-ascorbate. Extracts were thawed on ice, filtered through a 0.45-μm filter and chlorophylls were determined spectrophotometrically (V-1100, J.P. Selecta, Abrera, Spain) according to Lichtenthaler (1987).

Statistical analysis

Data are expressed as means ± standard error of the mean. One-way analyses of variance were performed to identify the leaf age effect on each of the measured traits. Multiple comparisons were carried out among 0-, 1- and 2-year-old leaves using the post hoc Tukey's honestly significant difference test. Student's *t*-tests were used to compare current-year leaves (0-year-old) measured in September 2018 with 2-year-old leaves measured in September 2020 to evaluate the changes of the measured traits due to leaf aging within the same cohort of leaves. Principal components analysis (PCA) was used to summarize the multivariate relationships among the measured traits of 0-, 1- and 2-year-old leaves. All statistical analyses were performed in the R software environment (version 4.0.0, R Development Core Team 2018).

Results

For measurements performed both in 2018 and in 2020, all photosynthetic characteristics decreased with increasing leaf

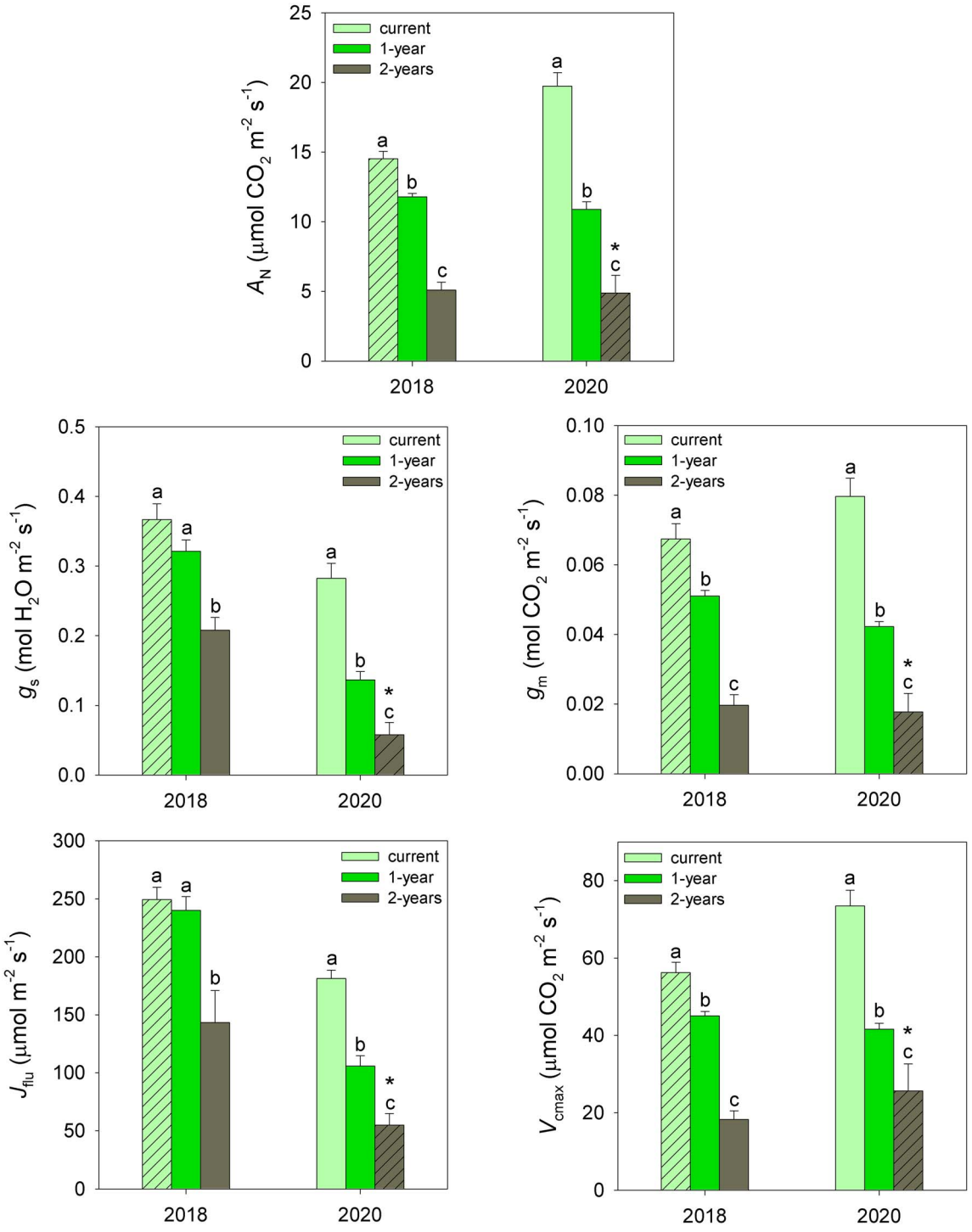

Figure 1. Photosynthetic characteristics for 0- (current), 1- and 2-year-old leaves of *Q. ilex* subsp. *rotundifolia* measured in 2018 and 2020: A_N, net assimilation rate; g_s, stomatal conductance; g_m, mesophyll conductance; J_{flu}, photosynthetic electron transport rate; V_{cmax}, maximum velocity of carboxylation. Data are means ± SE. Different letters indicate significant differences among 0-, 1- and 2-year-old leaves (Tukey's test, $P < 0.05$). Asterisks indicate significant differences between current-year leaves measured in 2018 and 2-year-old leaves measured in September 2020 (striped bars) (Student's *t*-test, $P < 0.05$).

age within the individual branches (Figure 1). In addition, for the same cohorts of leaves measured in two different years (0-year-old leaves in 2018 and 2-year-old leaves in 2020), leaf photosynthetic traits were also greater in 0-year-old leaves measured in 2018 than in 2-year-old leaves measured in 2020 (Figure 1). Analogously, leaf nitrogen concentration (N) decreased with increasing leaf age, although exclusively in terms of nitrogen allocated in the cytoplasm (Figure 2). The LMA varied less, and only the current-year leaves measured in 2018 had a lower LMA than 1- and 2-year-old leaves (Figure 2).

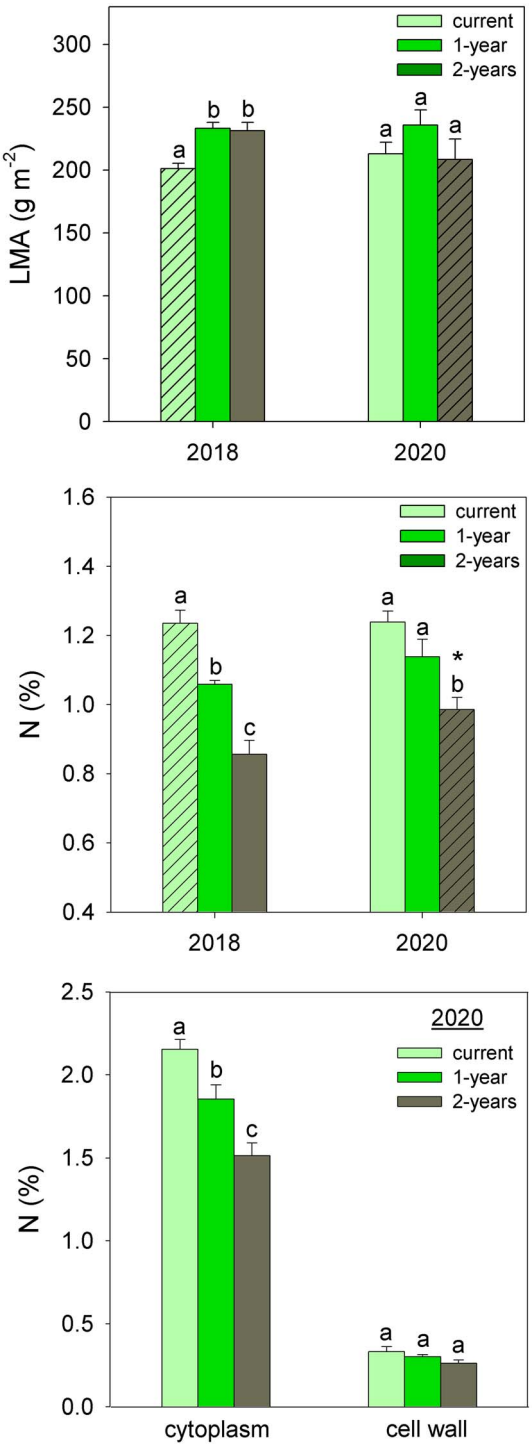

Figure 2. Leaf mass per area (LMA) (upper panel) and total leaf nitrogen concentration (N) on mass basis (medium panel) for 0- (current), 1- and 2-year-old leaves of *Q. ilex* subsp. *rotundifolia* measured in 2018 and 2020. Lower panel shows cytoplasmic and cell wall N concentrations on mass basis for 0- (current), 1- and 2-year-old leaves of *Q. ilex* subsp. *rotundifolia* measured in 2020. Data are means ± SE. Different letters indicate significant differences among 0-, 1- and 2-year-old leaves (Tukey's test, $P < 0.05$). Asterisk indicates significant differences between current-year leaves measured in 2018 and 2-year-old leaves measured in September 2020 (striped bars) (Student's *t*-test, $P < 0.05$).

Leaf age-dependent differences in net assimilation rate (A_N) were primarily driven by mesophyll conductance (g_m) and maximum velocity of carboxylation (V_{cmax}). Thus, the correlations between A_N and g_m ($r^2 = 0.94$, $P < 0.001$) and between A_N and V_{cmax} ($r^2 = 0.91$, $P < 0.001$) were stronger than those found between A_N and g_s ($r^2 = 0.32$, $P < 0.001$) and between A_N and J_{flu} ($r^2 = 0.26$, $P < 0.001$) (Figure 3). Analysis of the partitioning of photosynthetic limitations further confirmed that A_N was mainly limited by g_m and the relative importance of mesophyll limitation (l_m) increased with leaf age ($P < 0.05$, Figure S3 available as Supplementary data at *Tree Physiology* Online). A_N ($r^2 = 0.40$, $P < 0.001$) and V_{cmax} ($r^2 = 0.36$, $P < 0.001$) increased with increasing N concentration on area basis (Figure 4). No significant correlations were found between LMA and A_N and between LMA and N ($P > 0.01$, Figure 4).

Two-year-old leaves had a lower chloroplast surface area facing intercellular air spaces (S_c/S) than current and 1-year-old leaves (Figure 5). Moreover, S_c/S for 2-year-old leaves measured in 2020 was much lower than that for 0-year-old leaves measured in 2018 (Student's *t*-test, $P < 0.05$) (Figure 5). This primarily reflected presence of fewer chloroplasts in older leaves (Figure 6). Furthermore, a sharp decrease in the percentage of functional area per chloroplast was observed in 2-year-old leaves, both in 2018 and 2020, mainly due to a strong increase in the size of starch grains and plastoglobuli (Figures 6 and 7). The percentage of functional area per chloroplast was also lower for 2-year-old leaves measured in 2020 than in current-year leaves measured in 2018 (Figure 7). Cell wall thickness (T_{cw}) was greater in 2-year-old leaves than in 0- and 1-year-old leaves both in 2018 and 2020 (Figure 5). There were no age-related changes in chloroplast thickness (T_{chl}) (Figure 5). Mesophyll surface area facing intercellular air spaces per leaf area (S_m/S) also did not differ among leaf cohorts, except for a higher value in 0-year-old than in 1- and 2-year-old leaves measured in 2018 (Figure 5). T_{cw}, T_{chl} and S_m/S did not display significant differences between 0-year-old leaves measured in 2018 and 2-year-old leaves measured in 2020 (Figure 5).

Across leaf ages, a strong positive relationship was observed between S_c/S and A_N ($r^2 = 0.61$, $P < 0.001$) and a negative relationship between T_{cw} and A_N ($r^2 = 0.39$, $P < 0.05$) (Figure 8). No correlations were detected between T_{chl} and S_m/S and A_N ($P > 0.05$, Figure 8). A positive linear relationship was observed between measured values of g_m (Eq. (1)) and g_m values modeled using leaf anatomical traits ($g_{m,a}$, Eq. (3)) ($r^2 = 0.44$, $P < 0.001$, Figure S4 available as Supplementary data at *Tree Physiology* Online). Together with the correlations of A_N with S_c/S and T_{cw} (Figure 8), this underscores the importance of leaf anatomy in determining the differences in g_m and A_N among the different leaf age classes in *Q. ilex* subsp. *rotundifolia*.

In the PCA, the first and second principal components accounted for 53% and 15% of the total variation (Figure S5

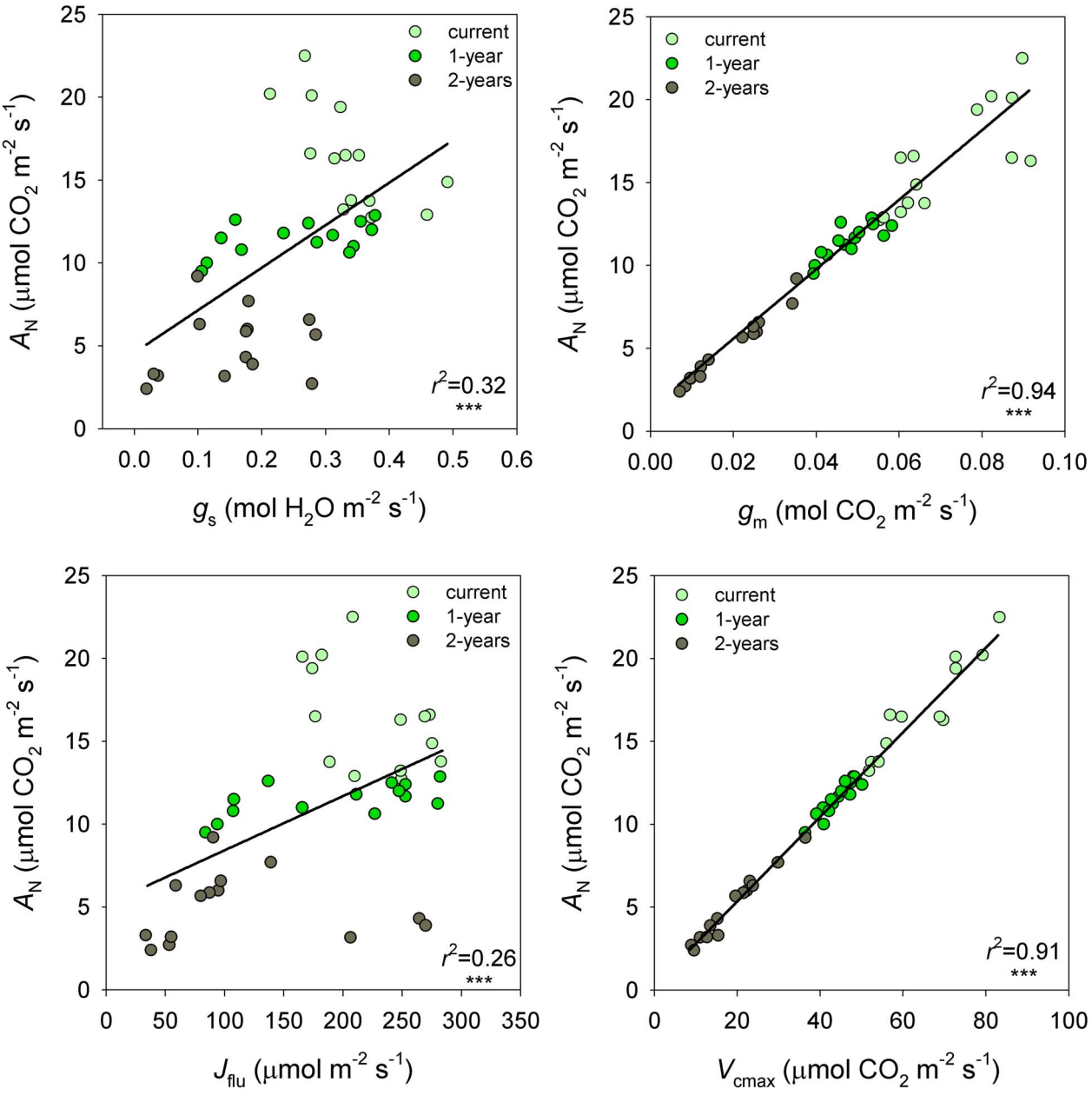

Figure 3. Relationships between net assimilation rate (A_N) and (i) stomatal conductance (g_s) (upper left panel), (ii) mesophyll conductance (g_m) (upper right panel), (iii) photosynthetic electron transport rate (J_{flu}) (lower left panel) and (iv) maximum velocity of carboxylation (V_{cmax}) (lower right panel) for 0- (current), 1- and 2-year-old leaves of *Q. ilex* subsp. *rotundifolia* measured in 2018 and 2020. ***$P < 0.001$.

available as Supplementary data at *Tree Physiology* Online). The first component integrated the variation in A_n, positively associated with g_m, S_c/S, V_{cmax} (and, to a lesser extent, N, g_s and J_{flu}), but negatively associated with T_{cw}. Conversely, the second component was not related with A_n, but showed positive weights for S_m/S and T_{chl}, and negative weights for g_s and J_{flu}. The scores of the studied leaf cohorts in the PCA biplot indicated that the functional and anatomical traits analyzed clearly differentiated 0-, 1- and 2-year-old leaves of *Q. ilex* subsp. *rotundifolia*. In particular, the three leaf age classes differed clearly along the first component (A_n and associated traits), whereas the second component explained the variability within each leaf cohort.

Discussion

Our study demonstrated a major decline in the photosynthetic activity with leaf age in *Q. ilex* subsp. *rotundifolia*, an evergreen Mediterranean oak with long leaf lifespan (Figure 1). Thus, this work agrees with the previous findings for this species by Escudero and Mediavilla (2003) and Niinemets et al. (2005, 2006). Furthermore, we have established a clear link between

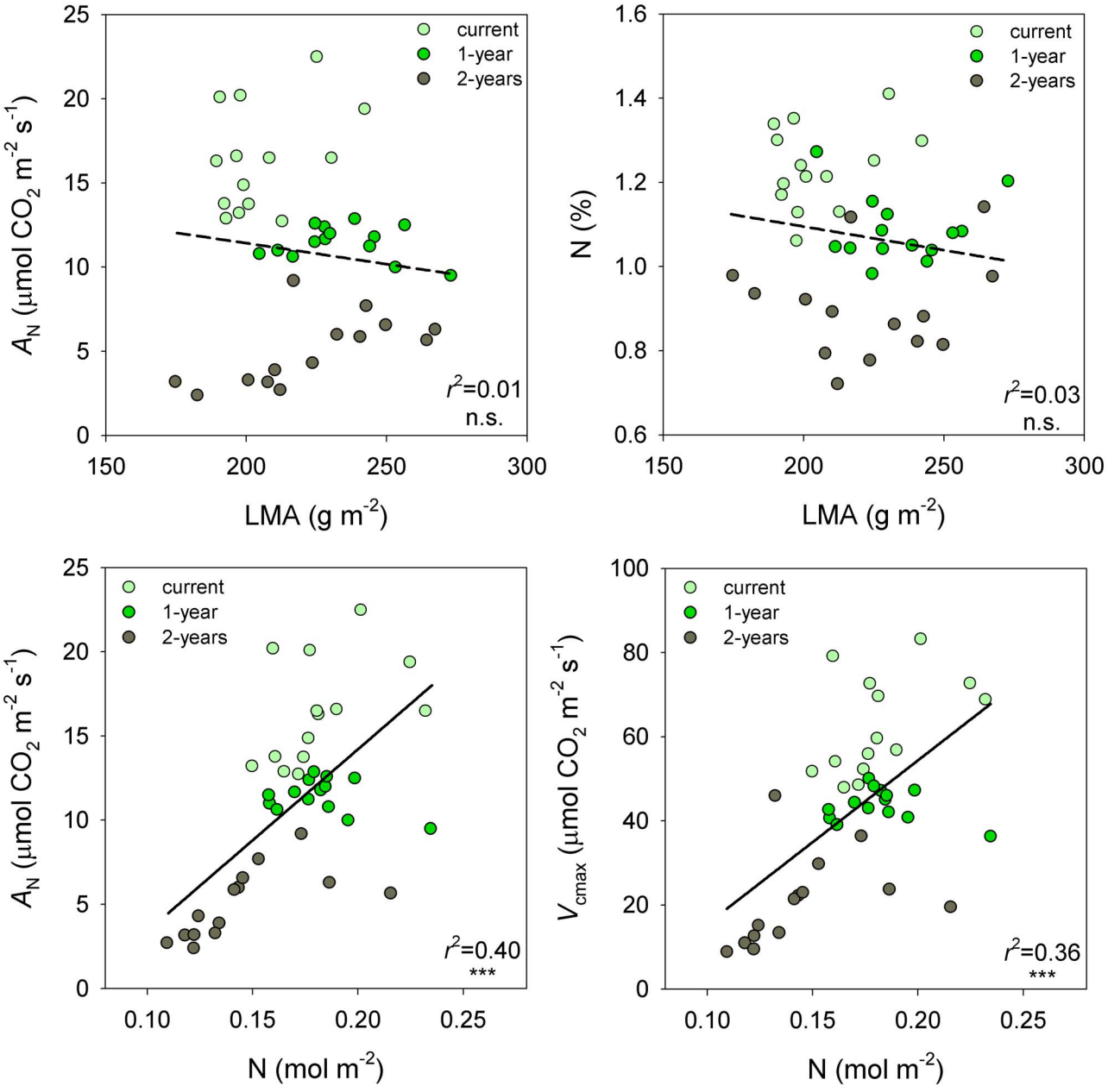

Figure 4. Relationships between LMA and (i) net assimilation rate (A_N) (upper left panel) and (ii) total leaf nitrogen concentration (N) on mass basis (upper right panel) for 0- (current), 1- and 2-year-old leaves of *Q. ilex* subsp. *rotundifolia* measured in 2018 and 2020. Relationships between total leaf nitrogen concentration (N) on area basis and (iii) net assimilation rate (A_N) (lower left panel), and (iv) maximum velocity of carboxylation (V_{cmax}) (lower right panel) for 0-, 1- and 2-year-old leaves of *Q. ilex* subsp. *rotundifolia* measured in 2018 and 2020. N.s. means non-significant relationship ($P > 0.05$). ***$P < 0.001$.

the decrease in A_N and the changes in g_m experienced by the different leaf cohorts (Figure 3) as indicated by Niinemets et al. (2005) for some Mediterranean evergreen tree species. This link has been also evidenced for *Q. ilex* subsp. *rotundifolia* when describing the within-species variation in g_m and A_N (Peguero-Pina et al. 2017*b*) and the response of these traits to water stress (Peguero-Pina et al. 2018, Alonso-Forn et al. 2021). In fact, the results here obtained support the idea that A_N was mainly limited by g_m and the relative importance of mesophyll limitation (l_m) increased with increasing leaf age ($P < 0.05$, Figure S3 available as Supplementary data at *Tree Physiology* Online).

The good relationship between modeled and measured g_m (Figure S4 available as Supplementary data at *Tree Physiology* Online) largely underpins a predominant role of anatomical traits in determining photosynthetic differences among different leaf age classes in *Q. ilex* subsp. *rotundifolia*. However, it should be noted that g_m measured with the Harley et al. (1992)

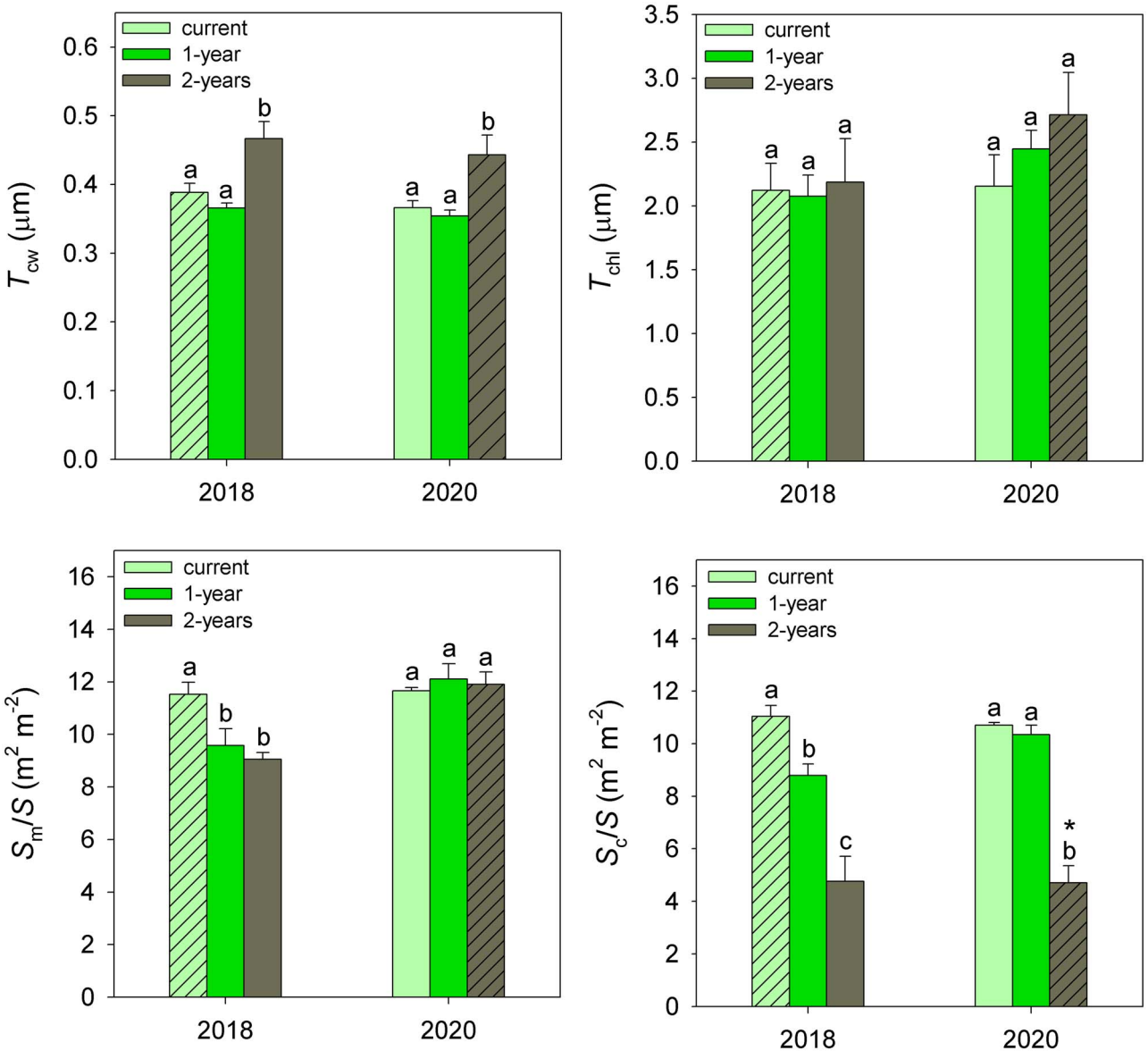

Figure 5. Cell wall thickness (T_{cw}), chloroplast thickness (T_{chl}) and mesophyll (S_m/S) and chloroplast (S_c/S) surface area facing intercellular air spaces per leaf area for 0- (current), 1- and 2-year-old leaves of *Q. ilex* subsp. *rotundifolia* measured in 2018 and 2020. Data are means ± SE. Different letters indicate significant differences among 0-, 1- and 2-year-old leaves (Tukey's test, $P < 0.05$). Asterisk indicates significant differences between current-year leaves measured in 2018 and 2-year-old leaves measured in September 2020 (striped bars) (Student's *t*-test, $P < 0.05$).

method was higher than g_m modeled with anatomical traits, which is contrary to expectations as modeled g_m usually gives the maximum theoretical value. This fact suggests the existence of other factors that might also influence the age-dependent changes in g_m displayed by *Q. ilex* subsp. *rotundifolia*. In this regard, Roig-Oliver et al. (2021) demonstrated that short-term changes in cell wall composition (i.e., pectins enhancement) were associated with g_m decline under water deficit in *Helianthus annuus* L. Therefore, it would be possible that long-term changes in cell wall composition might affect cell wall conductance and photosynthesis in *Q. ilex* subsp. *rotundifolia*, although this is a matter that deserves further investigation. In any case, regarding leaf anatomy, the reduction of both g_m and A_N in older leaves of this species was clearly induced by increases in cell wall thickness (T_{cw}) and reductions in chloroplast surface area exposed to intercellular air space per unit leaf area (S_c/S) (Figures 8 and S5 available as Supplementary data at *Tree Physiology* Online). To the extent of our knowledge, this is the first study that provides empirical evidence demonstrating changes in ultrastructural leaf anatomical traits as the explanation for the drawdown of photosynthesis and g_m with leaf age in species with high leaf longevity. Concerning cell wall thickness, Sugiura et al. (2020) stated that the decrease in g_m in old senescing leaves of *Glycine max* and *Phaseolus vulgaris* could

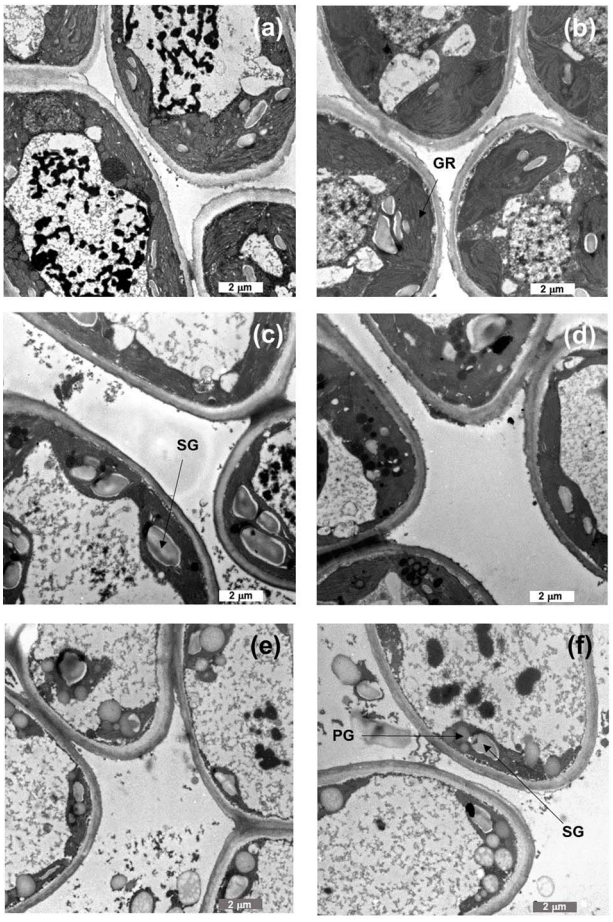

Figure 6. Transverse sections of 0- (current) (a, b), 1- (c, d) and 2-year-old (e, f) leaves of *Q. ilex* subsp. *rotundifolia* measured in 2018 (a, c, e) and 2020 (b, d, f). GR, grana; SG, starch grain; PG, plastoglobulus. Bars, 2 μm.

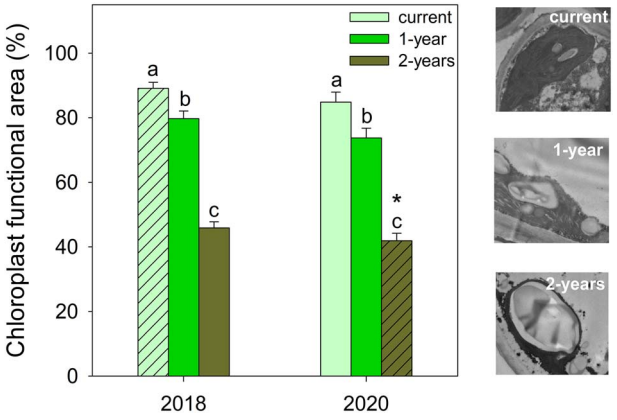

Figure 7. Functional area per chloroplast (%) for 0- (current), 1- and 2-year-old leaves of *Q. ilex* subsp. *rotundifolia* measured in 2018 and 2020. Data are means ± SE. Different letters indicate significant differences among 0-, 1- and 2-year-old leaves (Tukey's test, $P < 0.05$). Asterisk indicates significant differences between current-year leaves measured in 2018 and 2-year-old leaves measured in September 2020 (striped bars) (Student's *t*-test, $P < 0.05$). Micrographs located at the right of the panel show a representative chloroplast for each of the studied age classes.

be partly attributable to an increase in cell wall mass. Carriquí et al. (2021) also reported that leaf aging was associated with increases in T_{cw} in *Arabidopsis thaliana*, albeit without effects on g_m and photosynthesis probably due to a compensatory association between increased T_{cw} and decreased chloroplast thickness. Niinemets et al. (2005) suggested that the age-dependent increase in LMA in Mediterranean species reflected the higher investments in cell wall during leaf aging, with a concomitant effect on the CO_2 drawdown from internal air spaces to chloroplasts due to limited g_m. However, in our study, we only found minor changes in LMA among different leaf cohorts (Figure 2), and found no correlation between LMA and A_N (Figure 4). In addition, changes in T_{cw} during leaf aging, although correlated with A_N, were relatively small (Figures 8 and 9). By contrast, the stronger relationship found between A_N and S_c/S (Figure 8) demonstrated that S_c/S is the key anatomical trait dominating the variations in g_m and A_N among different leaf age classes in this species. Although the cell walls typically exert the strongest control on g_m (Peguero-Pina et al. 2017*a*, Veromann et al. 2017), other components such as S_c/S as observed in our study and in Veromann-Jürgenson et al. (2020), chloroplast thickness (Peguero-Pina et al. 2012) or the liquid-phase pathway length between cytosol and chloroplasts (Lei et al. 2021) can dominate changes in g_m. In fact, irrespective of the leaf age class, all T_{cw} values found in our study were relatively high, implying a major control on g_m (Terashima et al. 2011). However, the relative age-dependent change in T_{cw} was less than S_c/S, implying that age-dependent modifications in g_m were dominated by S_c/S in our study. Analogously, needle age-dependent reductions in g_m in three Mediterranean *Pinus* species were associated with reductions in S_c/S (Kuusk et al. 2018).

The reduction of S_c/S in old leaves may be related to the progressive dismantling of the photosynthetic apparatus associated to leaf aging (Niinemets et al. 2009, 2012). Chloroplast dismantling, i.e., the transition to the so-called 'gerontoplasts', is an essential process in leaf senescence that is characterized by ultrastructural changes such as the increase in size and number of plastoglobuli (Niinemets et al. 2012, Mulisch and Krupinska 2013, Domínguez and Cejudo 2021). In our study, chloroplasts in older leaves were characterized by a sharp decrease in their functional area (Figure 7), which could be associated to the size increase experienced by starch grains and plastoglobuli in 2-year-old leaves of *Q. ilex* subsp. *rotundifolia* (Figure 6). Leaf aging was also manifested in a decrease in total leaf nitrogen concentration, mainly in terms of nitrogen allocated in the cytoplasm of 2-year-old leaves (Figure 2). Consequently, it might be expected that the dismantling of the photosynthetic apparatus could have a strong impact on the amount of Rubisco, explaining the sharp decrease in V_{cmax}

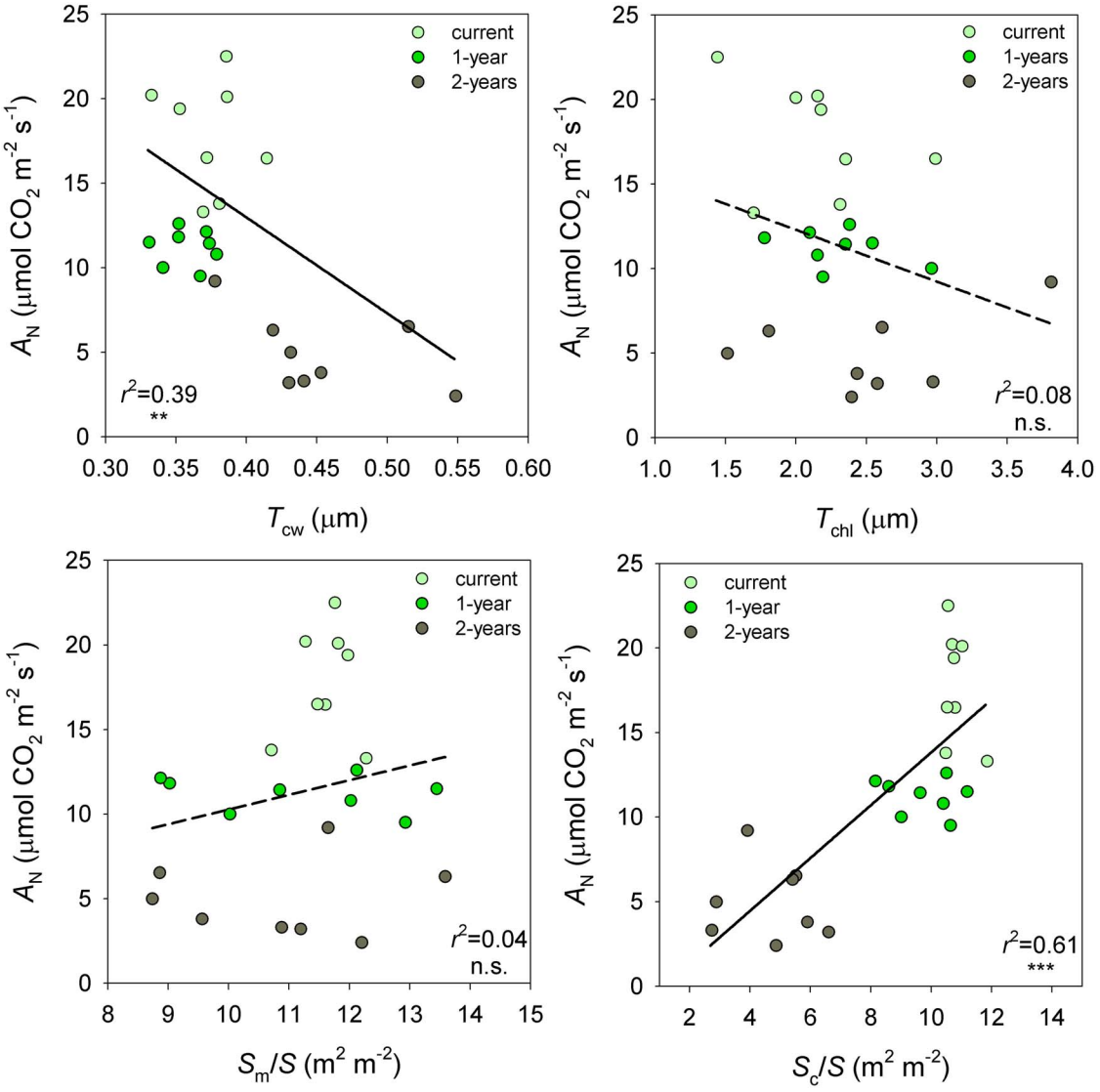

Figure 8. Relationships between net assimilation rate (A_N) and (i) cell wall thickness (T_{cw}) (upper left panel), (ii) chloroplast thickness (T_{chl}) (upper right panel), (iii) mesophyll surface area facing intercellular air spaces per leaf area (S_m/S) (lower left panel) and (iv) chloroplast surface area facing intercellular air spaces per leaf area (S_c/S) (lower right panel) for 0- (current), 1- and 2-year-old leaves of *Q. ilex* subsp. *rotundifolia* measured in 2018 and 2020. N.s. denotes a non-significant relationship ($P > 0.05$). $^{**}P < 0.05$. $^{***}P < 0.001$.

experienced by 2-year-old leaves (Figure 1), with a substantial impact on the photosynthetic capacity of this species (Figure 3 and 4).

At this point, the next question is, which is triggering the age-dependent decline of photosynthetic potential in *Q. ilex* subsp. *rotundifolia*? Different authors have argued that this could be the consequence of self-shading of older leaves within the crown as they age (Field and Mooney 1983, Kitajima et al. 1997, Ackerly 1999, Ishida et al. 1999, Niinemets et al. 2004, 2006, 2009). Thus, Terashima et al. (2005) stated that self-shading of older leaves might be involved in chlorophyll degradation and the regulation of leaf senescence. On the other hand, reacclimation of evergreen leaves to reduced light conditions is typically associated with increased chlorophyll content to harvest more light (Brooks et al. 1994, 1996). In addition, in these studies, chlorophyll a to b content also decreased upon reacclimation of older leaves after shading (Brooks et al. 1996), indicating a greater share of chlorophyll associated with the light harvesting complex II (Lichtenthaler et al. 2007). We observed a decrease in light availability in 1- and 2-year-old leaves with respect to current-year leaves of *Q. ilex* subsp. *rotundifolia* (Figures S1 and S2 available as Supplementary data at *Tree Physiology* Online), but without major consequences for the total amount of chlorophylls (Chl a + Chl b, Table S2 available as Supplementary data at *Tree Physiology* Online). However, contrary to other studies, the ratio Chl a/Chl b was higher in 2-year-old than in 1-year-old leaves (Table S2 available as Supplementary data at *Tree Physiology* Online), indicating

limited acclimation of pigment-protein complexes to altered light level but an acclimation to a higher light energy excess in *Q. ilex* subsp. *rotundifolia*.

Self-shading could also promote a decrease of nitrogen in older foliage due to the retranslocation from shaded to sunlit leaves (Hikosaka 2005). The concurrent decrease of A_N and nitrogen should imply the absence of changes in photosynthetic nitrogen-use efficiency (PNUE) with leaf age (Mooney et al. 1981, Field and Mooney 1983). However, in our study, we observed a strong decrease in PNUE with leaf age in *Q. ilex* subsp. *rotundifolia*, as demonstrated in other evergreen oak species (Escudero and Mediavilla 2003, Niinemets et al. 2004, Yasumura and Ishida 2011). This reflected a much greater decrease in net CO_2 assimilation than in leaf nitrogen content (Table S1 available as Supplementary data at *Tree Physiology* Online). Thus, this species has a substantial fraction of older leaves with an inherently low photosynthetic potential and nitrogen-use efficiency, irrespective of the amount of incident light (Table S1 available as Supplementary data at *Tree Physiology* Online). Despite this, 2-year-old leaves maintained a positive carbon balance, so the retention of these leaves would yield a higher whole-canopy net CO_2 assimilation despite their low PNUE and intrinsic water-use efficiency (iWUE = A_N/g_s) (Table S1 available as Supplementary data at *Tree Physiology* Online).

Besides self-shading, a possible increase in the allocation of nitrogen to cell walls with leaf age could also decrease photosynthetic activity and PNUE (Niinemets et al. 2009). A higher investment on cell wall biomass is expected to lead to an increase of LMA (Onoda et al. 2004). However, as stated above, we only found minor changes in LMA among different leaf cohorts (Figure 2), which was in line with the results obtained by Yasumura and Ishida (2011) for the evergreen oak *Quercus myrsinaefolia*. Moreover, we did not observe an increase in the nitrogen content per dry mass in the cell wall with leaf age (Figure 2), and T_{cw} did not show differences between the same cohort of leaves measured in 2018 (current-year) and in 2020 (2-year-old) (Figure 5).

Therefore, it is not well established the triggering factor for the age-dependent physiological deterioration evidenced by leaves of *Q. ilex* subsp. *rotundifolia*. In this regard, the role of leaf hydraulic conductance decline as the causing factor of photosynthetic decay in senescent leaves should be also considered. The role of leaf hydraulics in leaf senescence was suggested early by Neumann and Stein (1984), who hypothesized that the sequential pattern of leaf senescence observed during plant development in *P. vulgaris* L. may be related to progressive changes in the hydraulic architecture of the plant. Brodribb and Holbrook (2003) found a declining leaf hydraulic conductance that was probably linked to the loss of photosynthetic capacity during leaf senescence in two deciduous tree species (*Calycophyllum candidissimum* and *Rhedera trinervis*). In line with this, Locke and Ort (2014) showed that hydraulic decline in *G. max* during senescence was accompanied by gradual decreases in leaf water status and photosynthesis, although they could not conclude if this decline triggered photosynthetic decline and senescence. This mechanism was described by Giraldo et al. (2013), who proposed that the timing of leaf senescence in *Solanum lycopersicum* L. was determined by an age-dependent decline in leaf hydraulic conductance limiting gas exchange. However, these authors did not find evidence of this phenomenon in deciduous tree species such as *Acer saccharum* Marsh. and *Quercus rubra* L. In any case, to the best of our knowledge, no studies have dealt with this issue in evergreen trees with long leaf lifespan. More research is needed to clarify the possible involvement of leaf hydraulics decline in the age-dependent changes of photosynthetic capacity observed in *Q. ilex* subsp. *rotundifolia*.

Conclusions

In conclusion, our study demonstrates major age-dependent changes in leaf photosynthetic capacity that were driven by alterations in mesophyll conductance due to anatomical modification. However, the age-dependent decrease in the foliage photosynthetic potentials was weakly associated with self-shading and/or an increase in cell wall biomass. By contrast, confirming our hypotheses, we observed that changes in leaf anatomical (i.e., a strong decrease in S_c/S) and biochemical (i.e., a decrease in leaf nitrogen content and nitrogen investments in photosynthetic machinery) traits were responsible for the age-dependent modifications. These changes reflect a gradual physiological deterioration related to the dismantling of the photosynthetic apparatus. Further research is needed to elucidate the ultimate causing factor that triggers the physiological deterioration of leaves of evergreen trees with long leaf lifespan.

Authors' contributions

D.A.-F., J.J.P.–P., J.P.F., D.S.-K. and E.G.-P. planned and designed the research. D.A.-F., J.J.P.–P., J.P.F., R.M.-S. and D.S.-K. performed the experiments. D.A.-F., J.J.P.–P., J.P.F., J.I.G.-P., Ü.N., D.S.-K. and E.G-P. analyzed the data. D.A.-F., J.J.P.–P and E.G.-P. drafted the manuscript. All authors edited the manuscript with valuable inputs.

Supplementary data

Supplementary data for this article are available at *Tree Physiology* Online.

Funding

This research was funded by Grant PID2019-106701RR-I00 funded by MCIN/AEI/10.13039/501100011033 and by Gobierno de Aragón H09_20R research group. The work of D.A.-F. is supported by an FPI-INIA contract BES-2017-081208 and that of R.M.-S. is supported by a pre-doctoral Gobierno de Aragón scholarship.

Conflict of interest

None declared.

References

Ackerly D (1999) Self-shading, carbon gain and leaf dynamics: a test of alternative optimality models. Oecologia 119:300–310.

Alonso-Forn D, Peguero-Pina JJ, Ferrio JP, Mencuccini M, Mendoza-Herrer Ó, Sancho-Knapik D, Gil-Pelegrín E (2021) Contrasting functional strategies following severe drought in two Mediterranean oaks with different leaf habit: *Quercus faginea* and *Quercus ilex* subsp. *rotundifolia*. Tree Physiol 41:371–387.

Brodribb TJ, Holbrook NM (2003) Changes in leaf hydraulic conductance during leaf shedding in seasonally dry tropical Forest. New Phytol 158:295–303.

Brooks JR, Hinckley TM, Sprugel DG (1994) Acclimation responses of mature *Abies amabilis* sun foliage to shading. Oecologia 100:316–324.

Brooks JR, Sprugel DG, Hinckley TM (1996) The effects of light acclimation during and after foliage expansion on photosynthesis of *Abies amabilis* foliage within the canopy. Oecologia 107: 21–32.

Carriquí M, Roig-Oliver M, Brodribb TJ et al. (2019) Anatomical constraints to nonstomatal diffusion conductance and photosynthesis in lycophytes and bryophytes. New Phytol 222: 1256–1270.

Carriquí M, Nadal M, Flexas J (2021) Acclimation of mesophyll conductance and anatomy to light during leaf aging in *Arabidopsis thaliana*. Physiol Plant 172:1894–1907.

Cescatti A, Zorer R (2003) Structural acclimation and radiation regime of silver fir (*Abies alba* Mill.) shoots along a light gradient. Plant Cell Environ 26:429–442.

Chabot BF, Hicks DJ (1982) The ecology of leaf life spans. Annu Rev Ecol Evol Syst 13:229–259.

Clarke VC, Danila FR, von Caemmerer S (2021) CO_2 diffusion in tobacco: a link between mesophyll conductance and leaf anatomy. Interface Focus 11:20200040.

Corcuera L, Morales F, Abadía A, Gil-Pelegrín E (2005) Seasonal changes in photosynthesis and photoprotection in a *Quercus ilex* subsp. *ballota* woodland located in its upper altitudinal extreme in the Iberian peninsula. Tree Physiol 25:599–608.

De Kauwe MG, Lin Y-S, Wright IJ et al. (2016) A test of the 'one-point method' for estimating maximum carboxylation capacity from field-measured, light-saturated photosynthesis. New Phytol 210:1130–1144.

Domínguez F, Cejudo FJ (2021) Chloroplast dismantling in leaf senescence. J Exp Bot 72:5905–5918.

Escudero A, Mediavilla S (2003) Decline in photosynthetic nitrogen use efficiency with leaf age and nitrogen resorption as determinants of leaf life span. J Ecol 91:880–889.

Evans JR, von Caemmerer S, Setchell BA, Hudson GS (1994) The relationship between CO_2 transfer conductance and leaf anatomy in transgenic tobacco with a reduced content of rubisco. Aust J Plant Physiol 21:475–495.

Field C (1983) Allocating leaf nitrogen for the maximization of carbon gain: leaf age as a control on the allocation program. Oecologia 56:341–347.

Field C, Mooney HA (1983) Leaf age and seasonal effects on light, water, and nitrogen use efficiency in a California shrub. Oecologia 56:348–355.

Flexas J, Ortuño MF, Ribas-Carbo M, Diaz-Espejo A, Flórez-Sarasa ID, Medrano H (2007*a*) Mesophyll conductance to CO_2 in *Arabidopsis thaliana*. New Phytol 175:501–511.

Flexas J, Díaz-Espejo A, Berry JA, Galmés J, Cifre J, Kaldenhoff R, Medrano H, Ribas-Carbó M (2007*b*) Analysis of leakage in IRGA's leaf chambers of open gas exchange systems: quantification and its effects in photosynthesis parameterization. J Exp Bot 58:1533–1543.

Flexas J, Díaz-Espejo A, Gago J, Gallé A, Galmés J, Gulías J, Medrano H (2014) Photosynthetic limitations in Mediterranean plants: a review. Environ Exp Bot 103:12–23.

Freeland RO (1952) Effect of age of leaves upon the rate of photosynthesis in some conifers. Plant Physiol 27:685–690.

Galmés J, Andralojc PJ, Kapralov MV, Flexas J, Keys J, Molins A, Parry MAJ, Conesa MÀ (2014) Environmentally driven evolution of rubisco and improved photosynthesis and growth within the C3 genus *Limonium* (Plumbaginaceae). New Phytol 203: 989–999.

Genty B, Briantais JM, Baker NR (1989) The relationship between the quantum yield of photosynthetic electron transport and quenching of chlorophyll fluorescence. Biochim Biophys Acta 990: 87–92.

Giraldo JP, Wheeler JK, Huggett BA, Holbrook NM (2013) The role of leaf hydraulic conductance dynamics on the timing of leaf senescence. Funct Plant Biol 41:37–47.

Goering HK, Van Soest PJ (1970) Forage fiber analyses (apparatus, reagents, procedures, and some applications). US Government Publishing Office, Washington DC, USA.

Grassi G, Magnani F (2005) Stomatal, mesophyll conductance and biochemical limitations to photosynthesis as affected by drought and leaf ontogeny in ash and oak trees. Plant Cell Environ 28:834–849.

Harayama H, Ishida A, Yoshimura J (2016) Overwintering evergreen oaks reverse typical relationships between leaf traits in a species spectrum. R Soc Open Sci 3:160276.

Harley PC, Loreto F, Di Marco G, Sharkey TD (1992) Theoretical considerations when estimating the mesophyll conductance to CO_2 flux by analysis of the response of photosynthesis to CO_2. Plant Physiol 98:1429–1436.

Hikosaka K (2005) Leaf canopy as a dynamic system: ecophysiology and optimality in leaf turnover. Ann Bot 95:521–533.

Ishida A, Uemura A, Koike N, Matsumoto Y, Hoe AL (1999) Interactive effects of leaf age and self-shading on leaf structure, photosynthetic capacity and chlorophyll fluorescence in the rain forest tree, *Dryobalanops aromatica*. Tree Physiol 19:741–747.

Kikuzawa K (1991) A cost-benefit analysis of leaf habit and leaf longevity of trees and their geographical pattern. Am Nat 138:1250–1263.

Kitajima K, Mulkey SS, Wright SJ (1997) Decline of photosynthetic capacity with leaf age in relation to leaf longevities for five tropical canopy tree species. Am J Bot 84:702–708.

Krall JP, Edwards GE (1992) Relationship between photosystem II activity and CO_2 fixation in leaves. Physiol Plant 86:180–187.

Kuusk V, Niinemets Ü, Valladares F (2018) Structural controls on photosynthetic capacity through juvenile-to-adult transition and needle ageing in Mediterranean pines. Funct Ecol 32:1479–1491.

Lei Z, Liu F, Wright IJ et al. (2021) Comparisons of photosynthetic and anatomical traits between wild and domesticated cotton. J Exp Bot 73:873–885.

Lichtenthaler HK (1987) Chlorophylls and carotenoids: pigments of photosynthetic biomembranes. Methods Enzymol 148:350–382.

Lichtenthaler HK, Ac A, Marek MV, Kalina J, Urban O (2007) Differences in pigment composition, photosynthetic rates and chlorophyll fluorescence images of sun and shade leaves of four tree species. Plant Physiol Biochem 45:577–588.

Locke AM, Ort DR (2014) Leaf hydraulic conductance declines in coordination with photosynthesis, transpiration and leaf water status as soybean leaves age regardless of soil moisture. J Exp Bot 65:6617–6627.

Loreto F, di Marco G, Tricoli D, Sharkey TD (1994) Measurements of mesophyll conductance, photosynthetic electron transport and alternative electron sinks of field grown wheat leaves. Photosynth Res 41:397–403.

Mediavilla S, Escudero A (2003) Leaf life span differs from retention time of biomass and nutrients in the crowns of evergreen species. Funct Ecol 17:541–548.

Mooney HA, Field C, Gulmon SL, Bazzaz FA (1981) Photosynthetic capacity in relation to leaf position in desert versus old-field annuals. Oecologia 50:109–112.

Mulisch M, Krupinska K (2013) Ultrastructural analyses of senescence associated dismantling of chloroplasts revisited. In: Biswal B, Krupinska K, Biswal UC (eds) Plastid development in leaves during growth and senescence. Advances in photosynthesis and respiration (including bioenergy and related processes), vol. 36. Springer, Dordrecht, pp 307–335.

Neumann PM, Stein Z (1984) Relative rates of delivery of xylem solutes to shoot tissues: possible relationship to sequential leaf senescence. Physiol Plant 62:390–397.

Niinemets Ü, Keenan TF (2014) Photosynthetic responses to stress in Mediterranean evergreens: mechanisms and models. Environ Exp Bot 103:24–41.

Niinemets Ü, Reichstein M (2003) Controls on the emission of plant volatiles through stomata: a sensitivity analysis. J Geophys Res 108:4211.

Niinemets Ü, Tenhunen JD, Beyschlag W (2004) Spatial and age-dependent modifications of photosynthetic capacity in four Mediterranean oak species. Funct Plant Biol 31:1179–1193.

Niinemets Ü, Cescatti A, Rodeghiero M, Tosens T (2005) Leaf internal diffusion conductance limits photosynthesis more strongly in older leaves of Mediterranean evergreen broad-leaved species. Plant Cell Environ 28:1552–1566.

Niinemets Ü, Cescatti A, Rodeghiero M, Tosens T (2006) Complex adjustments of photosynthetic capacity and internal mesophyll conductance to current and previous light availabilities and leaf age in Mediterranean evergreen species *Quercus ilex*. Plant Cell Environ 29:1159–1178.

Niinemets Ü, Díaz-Espejo A, Flexas J, Galmés J, Warren CR (2009) Role of mesophyll diffusion conductance in constraining potential photosynthetic productivity in the field. J Exp Bot 60:2249–2270.

Niinemets Ü, García-Plazaola JI, Tosens T (2012) Photosynthesis during leaf development and ageing. In: Flexas J, Loreto F, Medrano H (eds) Terrestrial photosynthesis in a changing environment. A molecular, physiological and ecological approach. Cambridge University Press, Cambridge, UK, pp. 353–372.

Onoda Y, Hikosaka K, Hirose T (2004) Allocation of nitrogen to cell walls decreases photosynthetic nitrogen-use efficiency. Funct Ecol 18:419–425.

Peguero-Pina JJ, Camarero JJ, Abadía A, Martín E, González-Cascón R, Morales F, Gil-Pelegrín E (2007) Physiological performance of silver-fir (*Abies alba* Mill.) populations under contrasting climates near the south-western distribution limit of the species. Flora 202:226–236.

Peguero-Pina JJ, Flexas J, Galmés J, Niinemets Ü, Sancho-Knapik D, Barredo G, Villarroya D, Gil-Pelegrín E (2012) Leaf anatomical properties in relation to differences in mesophyll conductance to CO_2 and photosynthesis in two related Mediterranean *Abies* species. Plant Cell Environ 35:2121–2129.

Peguero-Pina JJ, Sisó S, Fernández-Marín B, Flexas J, Galmés J, García-Plazaola JI, Niinemets Ü, Sancho-Knapik D, Gil-Pelegrín E (2016*a*) Leaf functional plasticity decreases the water consumption without further consequences for carbon uptake in *Quercus coccifera* L. under Mediterranean conditions. Tree Physiol 36: 356–367.

Peguero-Pina JJ, Sancho-Knapik D, Flexas J, Galmés J, Niinemets Ü, Gil-Pelegrín E (2016*b*) Light acclimation of photosynthesis in two closely related firs (*Abies pinsapo* Boiss. and *Abies alba* Mill.): the role of leaf anatomy and mesophyll conductance to CO_2. Tree Physiol 36:300–310.

Peguero-Pina JJ, Sisó S, Sancho-Knapik D, Díaz-Espejo A, Flexas J, Galmés J, Gil-Pelegrín E (2016*c*) Leaf morphological and physiological adaptations of a deciduous oak (*Quercus faginea* Lam.) to the Mediterranean climate: a comparison with a closely related temperate species (*Quercus robur* L.). Tree Physiol 36:287–299.

Peguero-Pina JJ, Sisó S, Flexas J, Galmés J, García-Nogales A, Niinemets Ü, Sancho-Knapik D, Saz MÁ, Gil-Pelegrín E (2017*a*) Cell level anatomical characteristics explain high mesophyll conductance and photosynthetic capacity in sclerophyllous Mediterranean oaks. New Phytol 214:585–596.

Peguero-Pina JJ, Sisó S, Flexas J, Galmés J, Niinemets Ü, Sancho-Knapik D, Gil-Pelegrín E (2017*b*) Coordinated modifications in mesophyll conductance, photosynthetic potentials and leaf nitrogen contribute to explain the large variation in foliage net assimilation rates across *Quercus ilex* provenances. Tree Physiol 37: 1084–1094.

Peguero-Pina JJ, Mendoza-Herrer Ó, Gil-Pelegrín E, Sancho-Knapik D (2018) Cavitation limits the recovery of gas exchange after severe drought stress in holm oak (*Quercus ilex* L.). Forests 9: 443.

R Development Core Team (2018) R: A language and environment for statistical computing. Vienna, Austria: R Foundation for Statistical Computing. Retrieved from http://www.R-project.org/.

Roig-Oliver M, Bresta P, Nikolopoulos D, Bota J, Flexas J (2021) Dynamic changes in cell wall composition of mature sunflower leaves under distinct water regimes affect photosynthesis. J Exp Bot 72:7863–7875.

Sáez P, Bravo LA, Cavieres LA, Vallejos V, Sanhueza C, Font-Carrascosa M, Gil-Pelegrín E, Peguero-Pina JJ, Galmés J (2017) Photosynthetic limitations in Antarctic vascular plants: importance of the leaf anatomical traits and rubisco kinetics parameters. J Exp Bot 68: 2871–2883.

Sáez PL, Cavieres LA, Galmés J et al. (2018) In situ warming in the Antarctic: effects on growth and photosynthesis in Antarctic vascular plants. New Phytol 218:1406–1418.

Sala i Serra A (1992) Water relations, canopy structure, and canopy gas exchange in a *Quercus ilex f*orest: variation in time and space. In: PhD Thesis. Universitat de Barcelona, Facultat de Biologia, Departament d'ecologia, Barcelona, Spain.

Smart CM (1994) Gene expression during leaf senescence. New Phytol 126:419–448.

Sugiura D, Terashima I, Evans JR (2020) A decrease in mesophyll conductance by cell-wall thickening contributes to photosynthetic downregulation. Plant Physiol 183:1600–1611.

Syvertsen JP, Lloyd J, McConchie C, Kriedemann PE, Farquhar GD (1995) On the relationship between leaf anatomy and CO_2 diffusion through the mesophyll of hypostomatous leaves. Plant Cell Environ 18:149–157.

Terashima I, Araya T, Miyazawa S-I, Sone K, Yano S (2005) Construction and maintenance of the optimal photosynthetic systems of the leaf, herbaceous plant and tree: an eco-developmental treatise. Ann Bot 95:507–519.

Terashima I, Hanba YT, Tholen D, Niinemets Ü (2011) Leaf functional anatomy in relation to photosynthesis. Plant Physiol 155:108–116.

Tholen D, Ethier G, Genty B, Pepin S, Zhu X (2012) Variable mesophyll conductance revisited: theoretical background and experimental implications. Plant Cell Environ 35: 2087–2103.

Thomas H, Stoddart JL (1980) Leaf senescence. Annu Rev Plant Physiol 31:83–111.

Tomás M, Flexas J, Copolovici L, et al. (2013) Importance of leaf anatomy in determining mesophyll diffusion conductance to CO_2 across species: quantitative limitations and scaling up by models. J Exp Bot 64:2269–2281.

Tosens T, Niinemets Ü, Vislap V, Eichelmann H, Castro-Díez P (2012) Developmental changes in mesophyll diffusion conductance and photosynthetic capacity under different light and water availabilities in *Populus tremula*: how structure constrains function. Plant Cell Environ 35:839–856.

Veromann L-L, Tosens T, Laanisto L, Niinemets Ü (2017) Extremely thick cell walls and low mesophyll conductance: welcome to the world of ancient living! J Exp Bot 68:1639–1653.

Veromann-Jürgenson L-L, Brodribb TJ, Niinemets Ü, Tosens T (2020) Variability in the chloroplast area lining the intercellular airspace and cell walls drives mesophyll conductance in gymnosperms. J Exp Bot 71:4958–4971.

Warren CR (2006) Why does photosynthesis decrease with needle age in *Pinus pinaster*? Trees 20:157–164.

Yasumura Y, Ishida A (2011) Temporal variation in leaf nitrogen partitioning of a broad-leaved evergreen tree, *Quercus myrsinaefolia*. J Plant Res 124:115–123.

Zhang SB, Hu H, Li ZR (2008) Variation of photosynthetic capacity with leaf age in an alpine orchid, *Cypripedium flavum*. Acta Physiol Plant 30:381–388.